CERN-ATS-Note-2011-021

2011-04-05

alessandra.lombardi@cern.ch

Alignment and Field Error Tolerance in Linac4

G. Bellodi, M. Eshraqi,M. Garcia Tudela,L. Hein, J.B. Lallement, S. Lanzone, A.M. Lombardi,P. Posocco, E. Sargsyan.

Keywords: Linac4

Summary

LINAC4 [1] is a linear accelerator for negative Hydrogen ions (H−), which will replace the 50 MeV proton LINAC (LINAC2) as linear injector for the CERN accelerators. The higher output energy (160 MeV) together with charge-exchange injection will allow increasing beam intensity in the following machines. LINAC4 is about 80 m long, normal-conducting, and will be housed in a tunnel 12 m below ground on the CERN Meyrin site. The location has been chosen to allow using LINAC4 as the first stage of acceleration for a Multi-MegaWatt superconducting LINAC (SPL [2]). A 60 m long transfer line brings the beam towards the present LINAC2-to-PS Booster transfer line, which is joined at the position of BHZ20. The new transfer line consists of 17 new quadrupoles, an RF cavity and 4 bending magnets to adjust both the direction and the level for injection into the PS Booster.
End-to-end beam dynamics simulations have been carried out in parallel with the codes PATH [3] and TRACEWIN[4]. Following the definition of the layout, statistical studies have been carried out in order to define the alignment tolerances and correction system that guarantee a radiologically safe operation at the highest beam duty cycle as well as the maximum level of RF phase and amplitude jitter the system can tolerate before beam quality at injection in the PS Booster - and later in the SPL- is compromised. In this paper we summarise the guidelines used to define the tolerances, the capability of the correction system and the final tolerances for all the elements of LINAC4.

Contents

1. LINAC4 layout

LINAC4 is a normal conducting linear accelerator operating at the frequency of 352MHz. The layout of LINAC4 is summarized in Table 1. The first element of LINAC4 is a RF volume source which provides a 400 μsec 80 mA H- beam at 45 keV with a repetition rate of 2 Hz. The first RF acceleration (from 45 keV to 3 MeV) is done by a 3 m long Radio Frequency Quadrupole. At 3 MeV the beam enters a 3.6 meter long chopper line, consisting of 11 quadrupoles, 3 bunchers and two sets of deflecting plates. The beam is then further accelerated to 50 MeV in a conventional Drift Tube LINAC (DTL). The DTL, subdivided in 3 tanks, is 19 meters long. Each of the 109 drift tubes is equipped with a Permanet Magnet Quadrupole (PMQ). The acceleration from 50 to 100 MeV is provided by a Cell-Coupled Drift Tube LINAC (CCDTL). The CCDTL is made of 21 tanks of 3 cells each for a total length of 25 meters. Three tanks are powered by the same klystron, and constitute a module. The focusing is provided by electromagnetic quadrupoles placed between each module and PMQ outside each tank. The acceleration from 100 to 160 MeV is done in a PI-Mode Structure. The PIMS is made of 12 tanks of 7 cells each for a total of 22 m. Focusing is provided by 12 Electromagnetic Quadrupoles (EMQ). The 160 MeV beam at the output of the PIMS is guided by 4 dipoles (2 horizontal and 2 vertical) to the location of BHZ20, the present switching magnet from the 50MeV LINAC2 beam to the PS Booster. The plane of the LINAC4 is infact 2.5 meters below the PS Booster and the angle between the LINAC4 and the present proton transfer line to the booster is 46 degrees. The present location of LINAC4 was chosen [5] to accommodate the possibility of further energy upgrades.

The integrated gradient of the 180 quadrupoles (2/3 of which are permanent quads) and the phase and amplitude of the 260 RF accelerating gaps are shown in Figures 1-3. The main beam parameters of LINAC4 are summarized in Table 2

Table 1: Elements of LINAC4

	LEBT	**RFQ**	**CHOPPER**	**DTL**	**CCDTL**	**PIMS**	**Transfer line**
Energy(MeV)	0.045	3	3	50	100	160	160
Length (m)	1.8	3	3.6	19	25	22	70 +100
RF		1 tank	3 cavities	3 tanks	21tanks	12 tanks	1 cavity
Focusing	2 Solen		11 EMQ	109 PMQ +4 PMQ (intertanks)	14 PMQ	12 EMQ	17 + 18 EMQ
				1EMQ	7 EMQ		
Correctors (Steerers)	2		2	2	4	6	13 + 10

Table 2: LINAC4 beam characteristics

	In parenthesis values for HP SPL
Ion species	**H^-**
Output kinetic energy	**160 MeV**
Bunch frequency	**352.2 MHz**
Max. repetition rate	**2.0 (50) Hz**
Beam pulse duration	**0.4 (1.2) ms**
Chopping factor (beam on)	**65%**
Source current	**80 mA**
LINAC current	**64 mA**
Average current during beam pulse	**40 mA**
Beam power	**2.8 kW**
Particles / pulse	**$1.0\ 10^{14}$**
Transverse emittance (source) Rms normalised	**0.25 mm mrad**
Transverse emittance (LINAC) Rms normalised	**0.35 mm mrad**

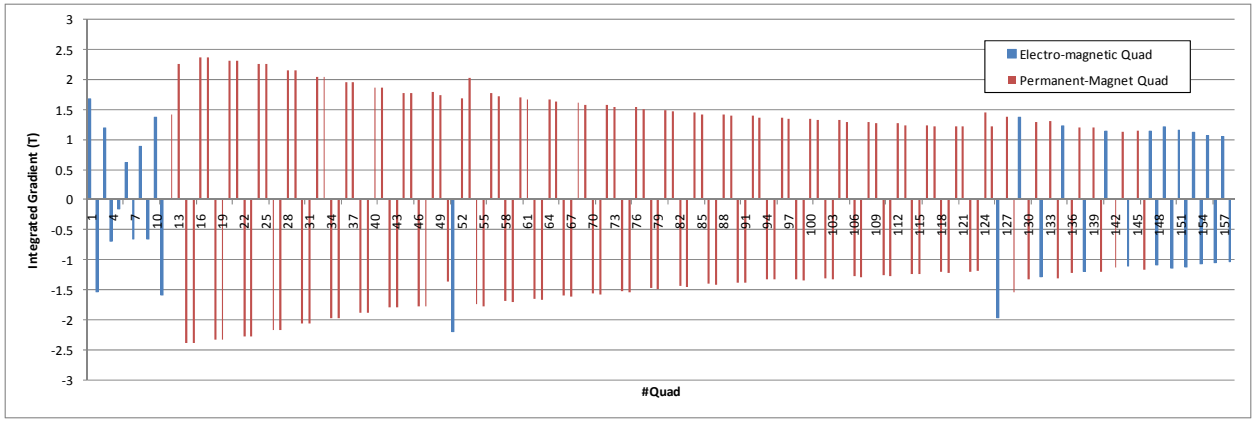

Figure 1: LINAC4 nominal quadrupole setting in the LINAC.

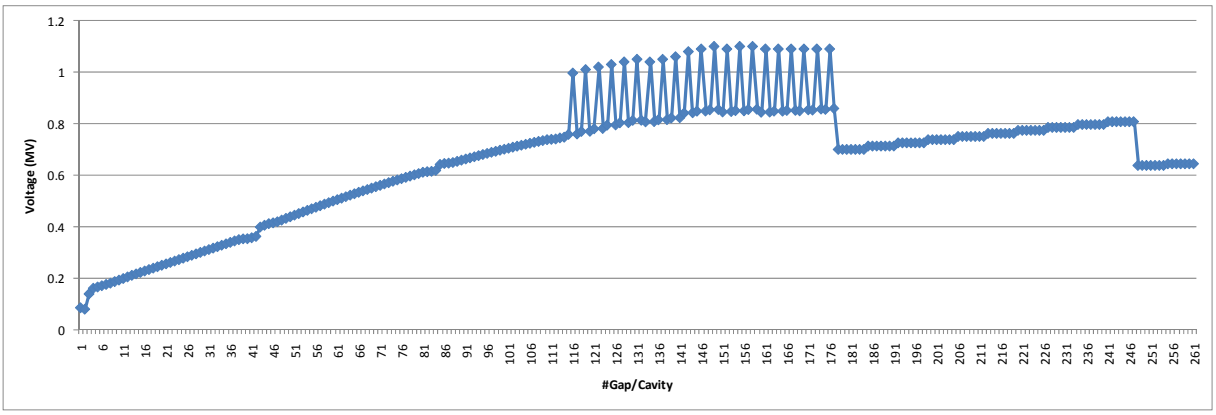

Figure 2: LINAC4 nominal RF gap effective voltage (EoTL)

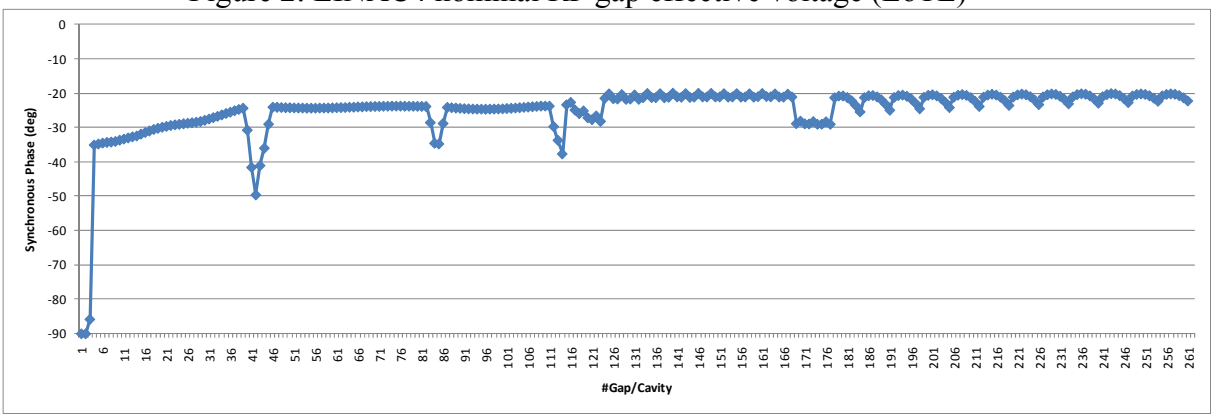

Figure 3: LINAC4 nominal RF phase setting

2. End-to-end simulation of LINAC4 with PATH and TRACEWIN

End-to-end simulations from the output of the source up to the stripping foil at booster injection have been performed both with TRACEWIN and PATH and results agree within few percent [6]. In the following only PATH results are reported unless otherwise indicated. The RFQ has been calculated both with TOUTATIS [7] and PARMTEQM [8]. A beam of 100K macro-particles has been generated at the source and has been tracked all the way through the LINAC and the transfer line.

2.1 Nominal beam dynamics

Details about nominal beam dynamics of the latest layout are reported in [6] and [9]. In this paragraph we briefly summarize the main topics. The evolution of the emittance along the LINAC under nominal conditions is shown in Figure 4; the losses are shown in Figure 5 and the ratio between aperture and the r.m.s. size is shown in Figure 6. Worth noticing is that both the emittance and the losses are constant after 3 MeV; that the chopper dump is the bottleneck of the low energy end and it is as well used to remove some halo particles from the beam to avoid activation at higher energies. Although the particle distribution has been generated at the source and transported to the booster, all the plots are presented in two parts for sake of clarity : the LINAC plot goes from the source to the end of the PIMS and the transfer line plot goes from the end of the PIMS to the injection foil into the booster.

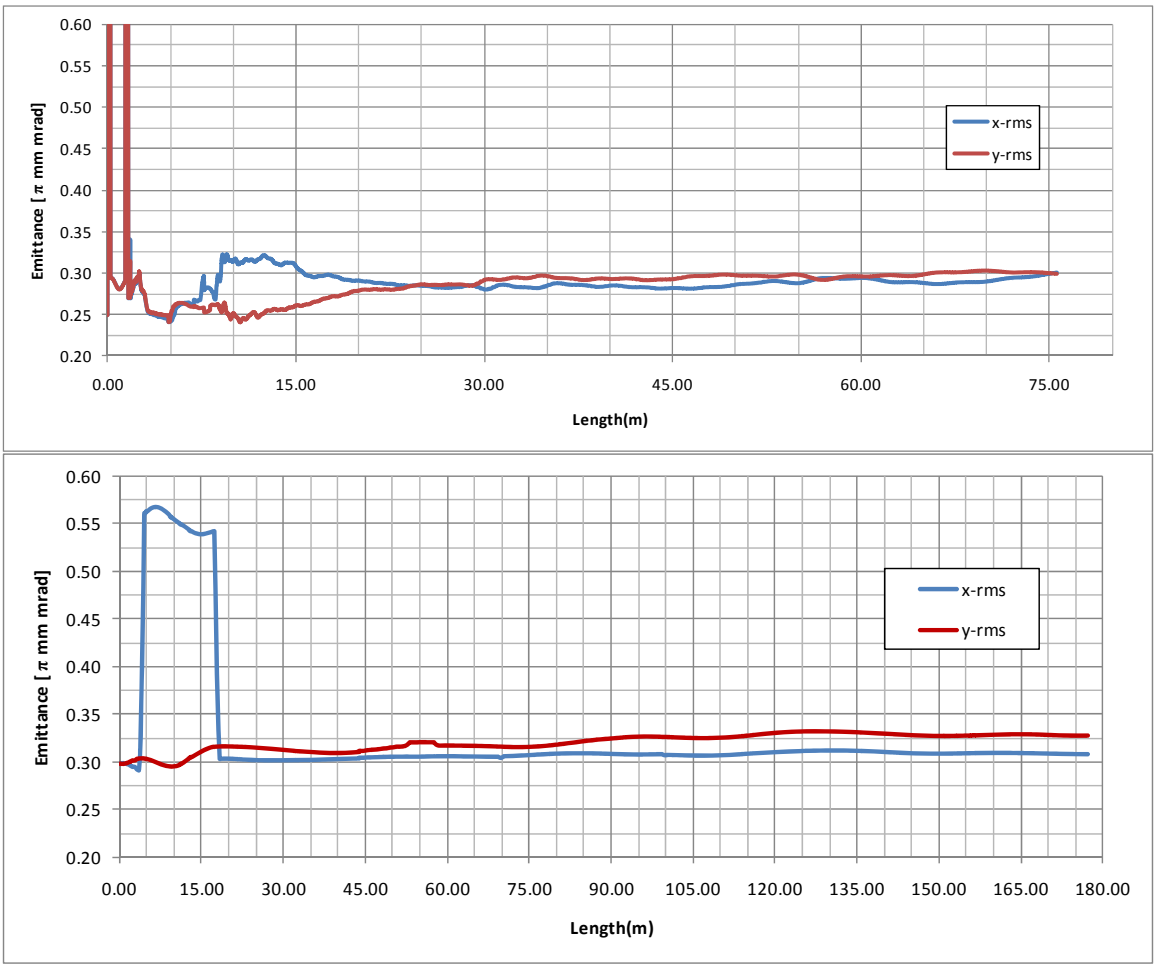

Figure 4: LINAC4 nominal transverse beam emittance evolution. Top: LEBT to PIMS output. Bottom: transfer lines.

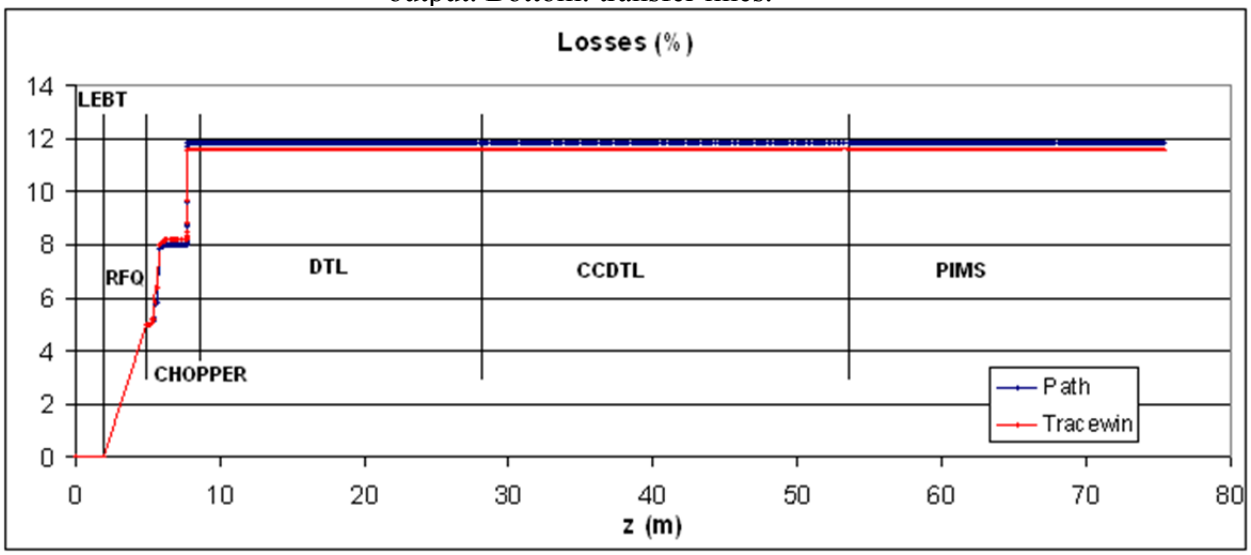

Figure 5: Losses in LINAC4 as predicted by two beam dynamics codes. There are no losses in the transfer lines, 8% is lost in the RFQ and 4 % in the chopper

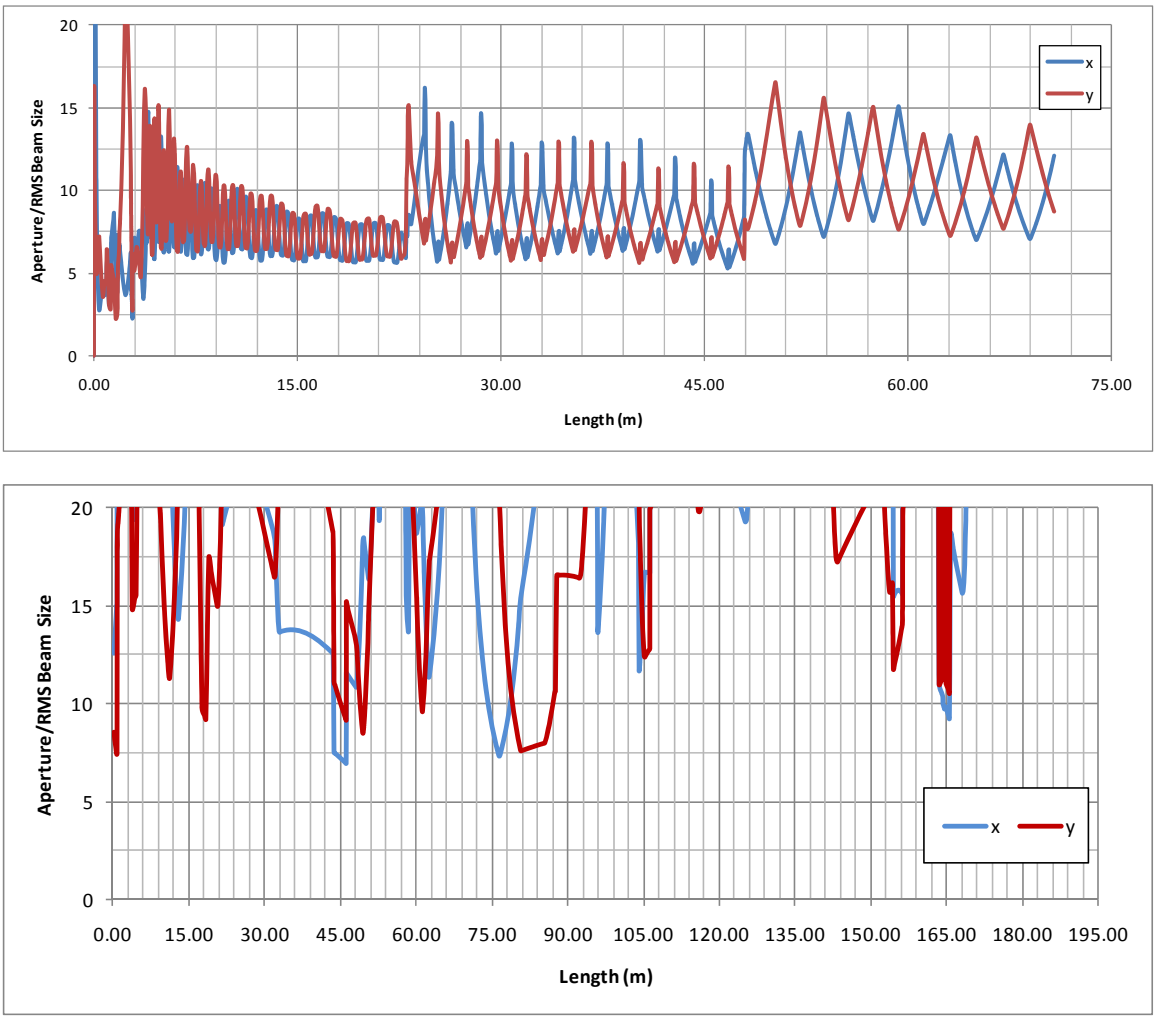

Figure 6: LINAC4 nominal aperture to r.m.s. beam size ratio. Top : MEBT to PIMS-output. Bottom : transfer lines.

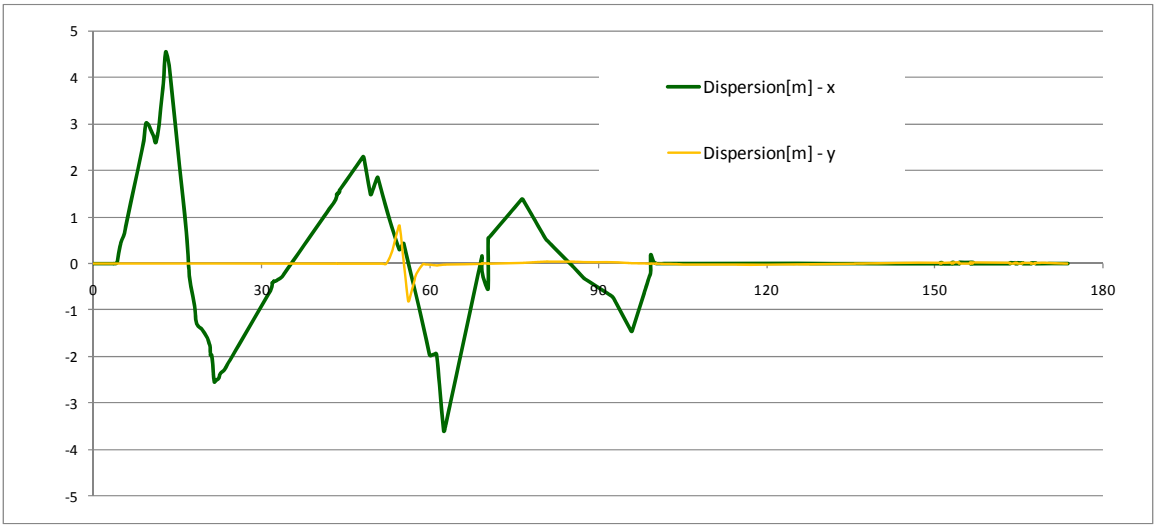

Figure 7: LINAC4 nominal dispersion, matched to 0 . z=0 corresponds to PIMS output, end of the plot is the stripper foil.

3. Errors

2.1 Method to evaluate the effect of errors

A campaign to define the alignment tolerances has been reported in [10].
In order to evaluate the effect of an error and to define tolerances a set of LINACs (typically 2000-5000) are generated with a statistical distribution of errors of the parameter being investigated. The distribution is chosen to be either a Gaussian cut at 3 sigmas or uniform, depending on the type of error. The relevant output beam parameters are recorded. A statistical analysis is performed on the relevant beam parameters observing the average, the minimum/maximum value and the standard deviation. Typically several values of the errors are tried, to identify an acceptable range and to find the value that should not be exceeded under any circumstance.
The parameter space of the possible errors and their combination is vast to say the least; therefore a series of preparatory runs has been performed to validate some short cuts, namely:

1) Combined effect of several errors on the same parameters: it has been verified that if the errors are un-correlated the effect of a several errors on the same parameters sum up (quadratically)
2) Cross talk longitudinal-transverse: in a LINAC the transverse and longitudinal plane are coupled both by space charge, RF defocusing and by the transverse components of the RF field. Nevertheless in first approximation it has been verified that "longitudinal errors" affect mainly energy and longitudinal emittance and that "transverse errors" affect mainly transverse emittance. Both errors have an effect on transmission.
3) Subparts of the machine can be run independently and the effect of the error propagated to the next section as an initial beam jitter.

The process of defining the tolerances from the results of an error study campaign is not always straightforward and it is a compromise between beam optics and a feasible and economical solution for error control. Often an "error budget" has to be shared amongst a series of potential sources of errors. Nevertheless a series of guidelines have been applied to define the tolerances which are:

1) The maximum allowed average losses at 5% duty cycle are 1 W/m in the LINAC. This requirement comes from the potential use of LINAC4 as a front end for a high power superconducting LINAC. This limit is not strictly applied in the transfer line to the PSB, as it is not foreseen to run the transfer line at higher than nominal duty cycle (0.08%).
2) The maximum allowed point-like loss (over 100 mm) is 0.1 W. This is somehow dictated by hand-on maintenance.
3) The transverse and longitudinal emittance growth should be limited to 20% (at 2 sigmas).
4) The phase and energy jitter should be compatible with injection into the booster including energy painting and dispersion induced transverse jitter.
5) The correction system should not in principle be used to correct for magnet alignment.

2.2 Static and dynamic errors

We distinguished two types of errors: static and dynamic. Static errors are constant or vary on a time scale of several days; amongst them we include alignment errors due to incorrect positioning, floor movements etc. Their effect is a constant degradation of the beam quality. Because they are stable in time their negative effect can be mitigated by a correction system. Conversely we call "dynamic" those errors that vary from bunch to bunch or from macro-pulse to macro-pulse. Those errors, which on average are zero, cause a jitter of beam parameters and/or an integrated beam degradation over time. The effect of these errors cannot be corrected. An example is the remnant RF amplitude jitter in a cavity after the feedback system has been applied.

The interpretation of the results of the statistics runs is different in the two cases. For static errors we should always prove that we are capable to cope (correct or accept) with the worst possible case. For dynamics errors we should prove that the degradation at two sigmas is within the boundary guidelines defined on page8.
Static errors turn out to be less dangerous than dynamic errors, as it will be shown in the following.

2.3 Alignment errors

We have applied 6 possible alignment errors to any active element. The errors are sketched in Figure 8. They include transverse position errors which represent the distance between the centre of the element and the ideal centre of the beam line in the two transverse planes and the longitudinal plane; and angle errors which represent the 3 angles between the ideal beam line reference and the reference system of the element. For magnets these values are referred to the magnetic centre i.e. they represent the 3 angles between the ideal beam line reference and the system in which the magnet is a perfect quadrupole. We have used a Gaussian distribution of the errors and have tried several values between ±0.1 and ±0.5 mm, ±0.2 to ±1 deg respectively. The effects of those errors are mainly increased beam losses, emittance growth and remnant coupling between planes. It has been found that longitudinal positioning errors are non-critical within the mm.

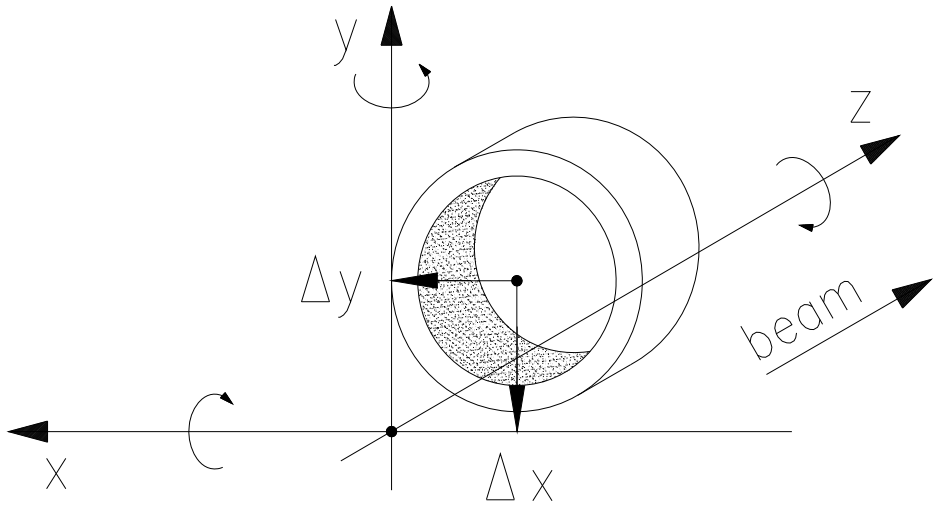

Figure 8 : Sketch showing the alignment errors applied to the quadrupoles.

2.4 Quadrupole field errors

We have applied gradient errors: they represent the percentage deviation from the nominal field. In the case of permanent magnet quadrupoles, they represent the accuracy to be reached when tuning the individual quadrupole; for electromagnets they represent the jitter of the field (from power supply). Each electromagnet, except few in the PIMS, is independently powered, so the errors are uncorrelated.

The results of the campaign has already been summarized in [10], a summary table defining the alignment tolerances is reported in chapter 4.

2.5 Chopping

Errors on the quadrupoles located in the line between the RFQ and the DTL will have an effect also on the efficiency of chopping as the quadrupole kick following the chopper is a key parameter in the beam separation at the inline chopper dump [11]. The quadrupoles concerned are L4L.MQD.3510, L4L.MQD.3610 and L4L.MQD.3710. For nominal values and nominal chopper voltage some 0.2% of the beam passes through the MEBT with chopper on. If the quadrupoles are varied around their nominal value by 10% the situation is the one reported in Figure 9: an unwanted transmission to the PS booster of up to 6% of the beam intensity can be possible. From this study we have confirmed the requirement of field error on the quadrupoles (±0.5% or better).

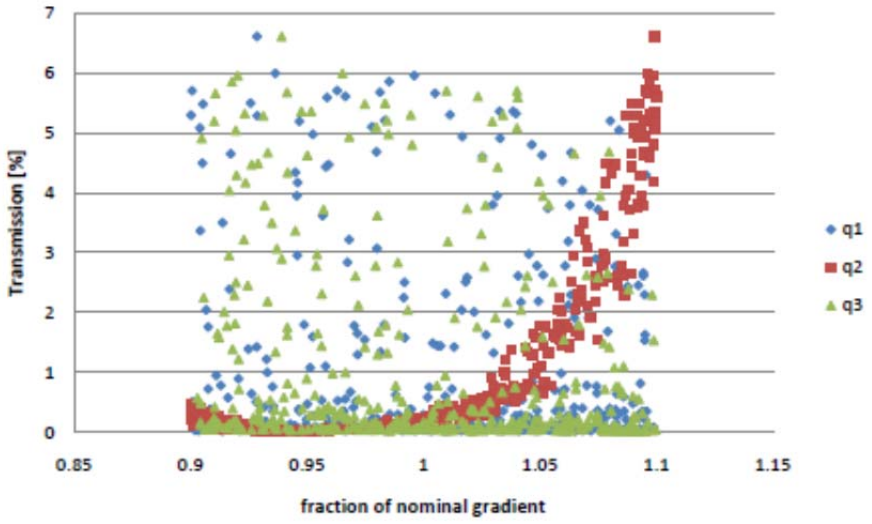

Figure 9 : Transmission to the PSB of un-chopped bunches as a function of quadrupole errors, uncorrelated errors between the three quadrupoles.

2.6 Bending field errors

We have applied field errors to the bending magnets in the new and old part of the transfer lines. The bending magnets in the new part are coupled to one power supply and consequently the errors are coupled. For sake of completeness we have analised also the effects of the individual errors. These errors represent the jitter of the power supply and their effect is to generate losses. Due to the long lever arm of the transfer lines the losses

are distributed all along the line and in severe cases they are concentrated in the line bottlenecks (septum and distributor). From Table 3 , we can define that the stability of the power supply should be of the order of 10^{-4} (in order to limit the losses to 1%)) and that the values of the bending current should be interlocked and limited to ±0.5-1% of the nominal value. This is comparable to what is in place nowadays on the LINAC2 (e.g. BHZ20 allowed value range is 1.5% around the nominal).

Table 3 : Losses induced by field error in each individual magnet of the transfer line

L4T.MBH.0150	percent error	losses
	0.4	50%
	0.35	25%
	0.32	10%
	0.3	5%
L4T.MBH.0350		1
	0.8	60%
	0.7	45%
	0.65	20%
	0.6	10%
	0.4	1%
	0.35	1%
	0.32	1%
	0.3	1%
L4T.MBV.1050		
	1.5	50%
	1.4	35%
	1.3	20%
	1.2	10%
	1.1	5%
	1.05	3%
	1	2%
	0.95	1%
	0.9	1%
	0.8	1%
	0.7	1%
	0.65	1%
	0.6	1%
	0.4	1%
	0.35	1%
	0.32	1%
	0.3	1%
L4T.MBV.1350		
	1.7	65%
	1.6	40%
	1.58	40%
	1.55	40%
	1.53	30%
	1.5	10%
	1.4	2%
	1.3	1%
	1.2	1%
	1.1	1%
	1	1%
BHZ20		
	1	100%
	0.8	70%

	0.7	40%
	0.65	30%
	0.6	16%
	0.55	6%
	0.5	2%
	0.4	1%
	0.3	1%
	0.2	1%
	0.1	1%
BHZ30		
	1	23%
	0.9	10%
	0.8	4%
	0.7	1%
	0.6	1%
	0.5	1%
	0.4	1%
L4T.MBH.0150/		I
L4T.MBH.0350	1	95%
	0.8	37%
	0.75	22%
	0.7	12%
	0.6	2%
	0.4	1%
L4T.MBV.1050/		
L4T.MBV.1350	10	100%
	8	99%
	7	75%
	6.9	60%
	6.6	14%
	6.3	2%

The data corresponding to the effect of an error in the vertical bending are graphed in Figure 10. The remarkable steep rise of the losses past the 1% error is due to the combined negative effect of the long lever arm (about 100m) between the vertical bending and the limited vertical aperture of the distributor (70 X 32 mm) and the phase advance inside the distributor. The values of table 3 are strongly dependent on the optics chosen and should be taken only as indication.

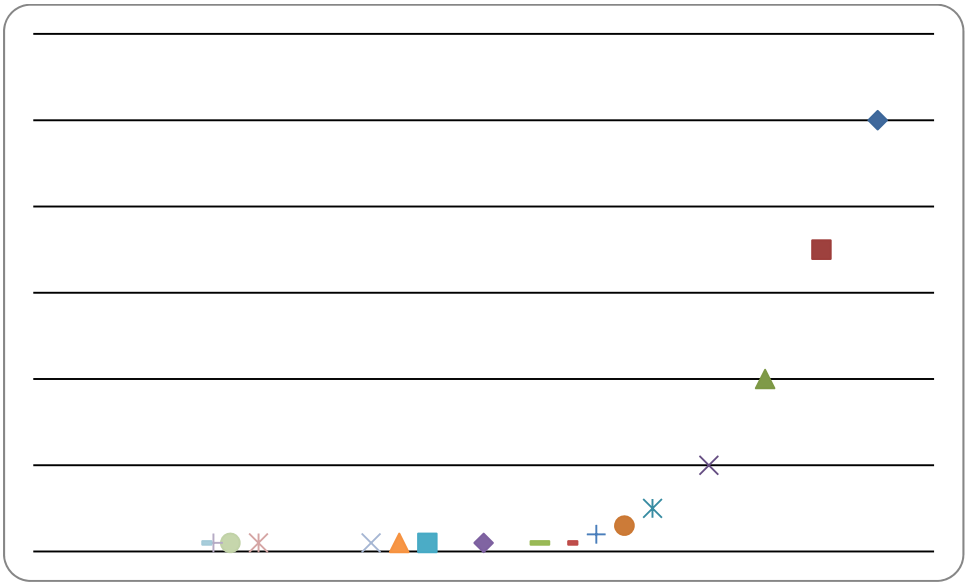

Figure 10 : Losses induced in transfer line vs. error in the vertical bending field.

2.7 Rf phase and amplitude errors

The RF distribution system of LINAC4 is described in [12]. A sketch is report below. Phase I is the starting phase, making use of LEP klystrons, whereas PhaseII corresponds to the time when the LEP Klystron will be replaced with 2.8 MW ones.

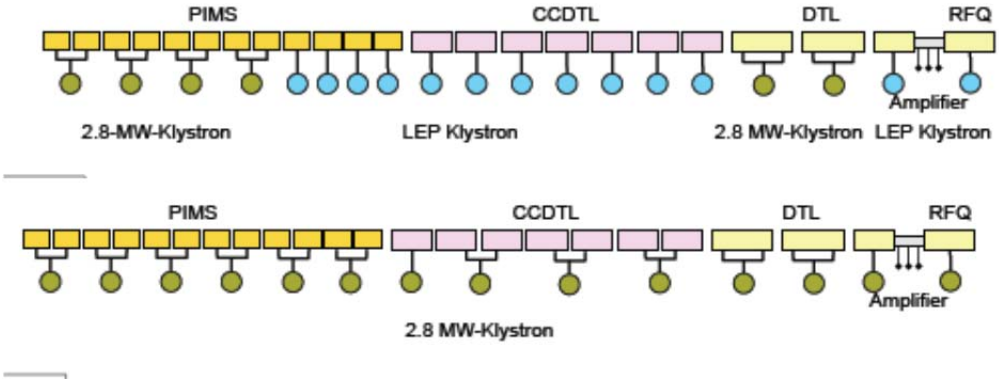

Figure 11 : RF power distribution scheme, Phase I (top) and Phase II (bottom).

For beam dynamics purposes the important quantity is the RF amplitude and phase at each accelerating gap. When several gaps are part of the same structure (DTL tanks, coupled tanklets in the CCDTL module) the phase at the first gap is determined by the klystron phase and at each following gap it is determined by the distance between the gap centre and the particle speed. The number of RF gaps coupled to the same power source is a critical input to the study; a summary is given in Table 4.

Table 4 : Number of RF gaps per klystron.

RFQ Klystron	300 gaps
DTL Klystrons (1,2,3)	36,42,30 gaps
CCDTL Klystrons	9 gaps or 18 gaps (phase II)
PIMS Klystrons	7 or 14 gaps

We have applied phase and amplitude errors to the RF structures. For each cavity or set of cavities on the same klystron we have generated an error on the beam arrival time in the cavity. This error entails a propagation of the oscillation of the phase (and energy) along all the RF gaps connected to the same power source and/or phase shifter. For each power source (klystron) we have assigned an amplitude error which affects by the same percentage all the rf gaps coupled to one power source.
As it can be seen from the sketch in Figure 11 some klystrons feed more than one cavity, their power divided via a power splitter. We have considered the case of unbalanced power splitting and evaluated its consequences for the CCDTL. We have assumed that the phase of each tank can be controlled independently. All the errors mentioned so far are considered to be "dynamic" errors, i.e. with variation from pulse to pulse or bunch-to-bunch. These errors affect mostly beam energy and phase jitter, and to a lesser degree the final value of the longitudinal emittance; they affect transmission only in extreme cases.

Besides the above mentioned errors we have evaluated the effects of "static" gap errors: they refer to random independent errors on rf gaps in the same cavity. They are –for example- tuning errors affecting field flatness or wanted field profile. They affect mainly the final longitudinal emittance and only in extreme case they affect the transmission. Their effect can be mitigated by increasing the RF power above nominal.

To evaluate the effect of the longitudinal errors a campaign of simulation including about 2000 error distributions per each case has been run. Errors in phase and amplitude are randomly generated within a uniform distribution. The errors are correlated (all the gaps on the same klystron have the same percentual error) when assessing the effects of klystron errors or uncorrelated (each gap has its own error) when assessing the effect of tuning imperfections. The runs were done in sequence (DTL, CCDTL, and PIMS) in order to include the effect of the input energy jitter due to the errors in the previous structure and reduce the number of runs. A comprehensive end-to-end run to verify the effect of the cumulative errors has been run only for few selected cases and it confirmed the prediction. For each run the transmission, longitudinal emittance, average phase (phase jitter) and average energy (energy jitter) was recorded and the error budget was assigned based on the acceptance of the following machine (phase and energy jitter, energy spread) and finally the acceptance of the PS Booster and the superconducting proton LINAC. In the following session the results of the study are reported in full. The final error budget for all cases is reported in chapter 5.

2.8 LINAC4 sensitivity to RF errors

For klystron errors we have considered values between ±0.5% and ±2% for the amplitude and values between ±0.5 and ±2 degrees for the phase. For tuning errors we have taken values from ±1% to ±10% depending on the cases.
We have also introduced a uniform input energy jitter coming from the previous stage of acceleration, which we estimate at 6KeV at the input of the DTL, 90 keV at the input of the CCDTL and 250 keV at the input of the PIMS. Those values (equivalent to a Gaussian distribution with a sigma of 2/3 the given value) turned out to be an overestimate of the results of the error studies. Some details in [13].

The results for the three accelerating structures (DTL, CCDTL and PIMS) are reported in the following. Unless explicitly mentioned, no effect on the transmission or on the transverse emittance was observed.

DTL sensitivity to Klystron errors (dynamic)

Table 5 : Effects of amplitude and phase jitter on the DTL output beam.

amplitude and phase	Phase jitter [deg] 1 sigma	Energy jitter [keV] 1 sigma	90% Emittance [deg MeV]	RMS Emittance [deg MeV]
nominal			0.734	0.167
±0.5% and ±0.5 deg	0.82	13	0.745±0.014	0.169±0.003
±0.5% and ±1 deg	0.88	18	0.751±0.017	0.171±0.004
±0.5% and ±2 deg	0.92	31	0.774±0.034	0.175±0.009
±1% and ±0.5 deg	1.6	23	0.757±0.024	0.171±0.005
±1% and ±1 deg	1.6	28	0.762±0.027	0.172±0.006
±1% and ±2 deg	1.83	36	0.786±0.047	0.177±0.011
±2% and ±0.5 deg	5.12	43	0.794±0.07	0.179±0.014
±2% and ±1 deg	5.66	46	0.799±0.07	0.180±0.017
±2% and ±2 deg	5.9	49	0.830±0.1	0.187±0.024

In Table 5 we report in detail the results of the effect of a klystron error on the beam phase and energy jitter and r.m.s. emittance at the end of the DTL. From the results we can deduce that the amplitude error has more effect than the phase errors and that a variation of ±2% in amplitude causes an emittance growth and an energy jitter above what is acceptable. A control of the amplitude and phase within ± 0.5% and ±0.5 degrees would be ideal but a control within ±1% and ±1 degree is also acceptable in the DTL.

DTL sensitivity to tuning errors (static)

The effects of the "static" errors were evaluated independently of the effects of the "dynamic" errors. In the 3 DTL tanks gap amplitude errors were assigned randomly and independently to the 112 gaps with a uniform distribution over ±1% to ±10% of the nominal voltage of each gap, and for each error distribution the average was corrected to match the nominal.

Table 6 : Effects of tuning errors on the DTL output beam.

	Transmission [%]	**Average Kinetic Energy [MeV]**	**100% Emittance [deg MeV]**	**90% Emittance [deg MeV]**	**RMS Emittance [deg MeV]**	
nominal	99.9977	49.98	10.45	0.734	0.167	
±1%	99.997±0.0009	49.98±0.020	11.82±3.24	0.774±0.010	0.168±0.02	Target value
±2%	99.997±0.0015	49.98±0.038	12.23±4.02	0.776±0.049	0.176±0.011	Acceptable
±5%	99.990±0.03	49.98±0.092	34.26±177.70	0.976±0.307	0.219±0.076	Halo develops
±10%	85	46±13	249±522	4.41±15	1.2±3.5	Affects Trans.

Table 6 shows that the DTL is quite forgiving of tuning errors, and errors up to ±2% can be accepted, provided enough RF power is available to bring the average field in each tank to the nominal value.

CCDTL sensitivity to Klystron errors (dynamic)

Table 7 : Effects of amplitude and phase jitter on the CCDTL output beam.

amplitude and phase	**Output phase jitter [deg] 1 sigma**	**Output energy jitter [keV] 1 sigma**	**90% Emittance [deg MeV]**	**RMS Emittance [deg MeV]**
nominal			0.769	0.196
±0.5% and ±0.5 deg	0.5	39	0.7713±0.013	0.196±0.003
±1% and ±1 deg	1	63	0.7732±0.018	0.196±0.005
±2% and ±2 deg	2	115	0.7801±0.030	0.198±0.009
±5% and ±2 deg	4	237	0.7939±0.047	0.200±0.015

Klystron phase and amplitude should be controlled ideally to ±0.5% ±0.5 deg to control energy and phase jitter at the CCDTL output but that a value of ±1% and ±1deg are still acceptable.

CCDTL sensitivity to tuning errors (static)

The ideal field distribution in a CCDTL module (3 Tanklets) is shown on Figure 12. A tilt over the three tanklets constituting a module has been simulated, and its effect on the beam at the output of the CCDTL is detailed in Table 8. An independent tilt, up to 2% and 5%, has been applied to all the 7 modules. The CCDTL is quite forgiving of field tilts, provided the average field over the module is adjusted to match the nominal.

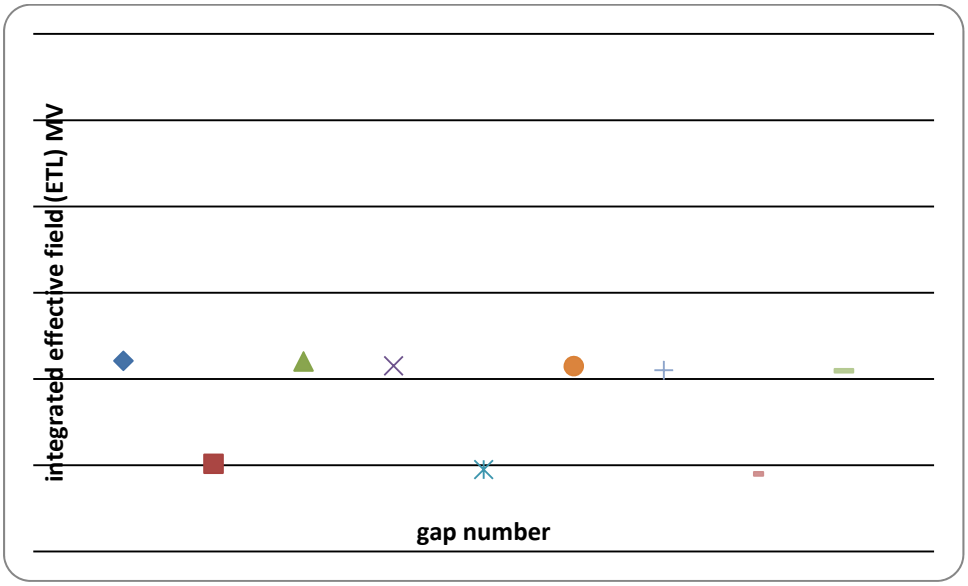

Figure 12: Ideal voltage distribution in one CCDTL module

Table 8 : Effects of tilt errors on the CCDTL output beam.

	Elong 90%,deg MeV	**Elong RMS, deg MeV**
nominal	0.769	0.196
2%	0.757±0.011	0.192±0.0025
5%	0.760±0.017	0.193±0.0044

CCDTL issues due to the powering scheme of Phase II

There are two issues that are specific to the powering scheme for Phase II shown in Figure 11 : the acceptable power unbalance between coupled modules and which module to leave unpaired. During Phase II the 7 CCDTL modules will be powered by 4 klystrons leaving the option of letting the first or last module powered by a single klystrons. The two issues are somehow coupled and they have therefore been studied together [13]. From now on we refer to the two powering scheme as "first module independent" and "last module independent". The "last module independent" is the baseline (Figure 11).

We have looked at average energy and longitudinal emittance increase both at the end of the CCDTL and at the end of the PIMS. Of course the cases are equivalent for perfect RF regulation. The sensitivity to RF errors is nevertheless different in the two cases and impact on the degradation of the longitudinal emittance and longitudinal mismatch to the PIMS is of concern.
We have applied a relative field difference between two coupled modules ranging from 5 to 15%; this error is static and it is assumed that the average field is correct but one

module has few percent less, the adjacent few percent more field. On top of this error we have applied a phase and amplitude jitter on the klystron, ±0.5% and ±0.5degrees respectively.

In general for any field difference between two coupled modules, the beam qualities are better if the first module is independently powered. This is explained by the fact that this module is part of the longitudinal matching between the DTL and the CCDTL. The effects are even amplified at the end of the PIMS.

In order to find a guideline on what module to leave independent, we have taken the problem under a different angle. We have fixed the maximum longitudinal emittance increase to 10% and deduced what is the maximum power splitting error for the two cases. We find that for the solution "last module independent" we need to have a better power splitting than for the solution "first module independent"(5% vs 10%).

Besides the above measures, the mismatch at the PIMS can be corrected by re-tuning all the phases in the CCDTL. The worst case found in the error studies could be corrected provided the phases could be controlled to ± 0.5deg.

The conclusion of the study is that if we keep the baseline solution "last module independent" we need to guarantee that the difference in cavity voltage between two coupled modules is better than 5% and that we regulate the phase precisely within ±0.5deg.

PIMS sensitivity to Klystron errors (dynamic)

Table 9 : Effects of amplitude and phase jitter on the PIMS output beam.

amplitude and phase	**Output Phase jitter [deg] 1 sigma**	**Output Energy jitter [keV] 1 sigma**	**90% Emittance [deg MeV]**	**RMS Emittance [deg MeV]**
nominal			0.740	0.180
±0.3% and ±0.3 deg	0.3	65.00	0.746±0.0045	0.181±0.00088
±0.5% and ±0.5 deg	0.4	78.00	0.746±0.0046	0.181±0.00094
±1% and ±1 deg	0.66	126.00	0.747±0.0053	0.181±0.0012
±2% and ±1 deg	0.85	220.00	0.747±0.0059	0.181±0.0013
±3% and ±1 deg		320.00	0.747±0.0069	0.181±0.0016

Klystron phase and amplitude should be controlled ideally to ±0.5% ±0.5 deg to control energy and phase jitter at the PIMS output. The transfer line energy jitter acceptance is 100 keV (1 sigma).

PIMS sensitivity to tuning errors (static)

The ideal field distribution in the PIMS is shown in Figure 13. The field is ideally constant inside each module. The last two modules are run at a lower nominal field in order to be able to raise them for the energy ramping within the pulse [13].

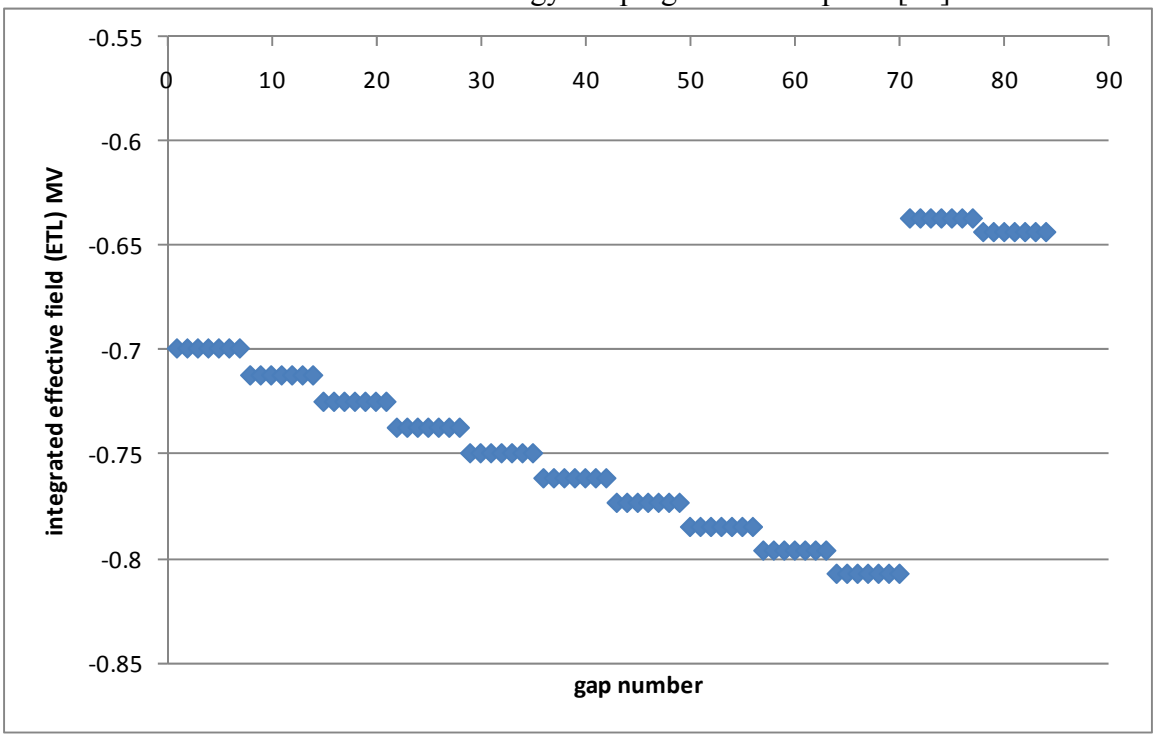

Figure 13: Ideal voltage distribution in the PIMS.

A series of runs has been performed to investigate the effects of a tilt (either elliptical or linear-see Figure 14), between the 7 identical gaps in a PIMS module. Table 10 shows the effects on the longitudinal emittance: tilts up to 5% are acceptable.

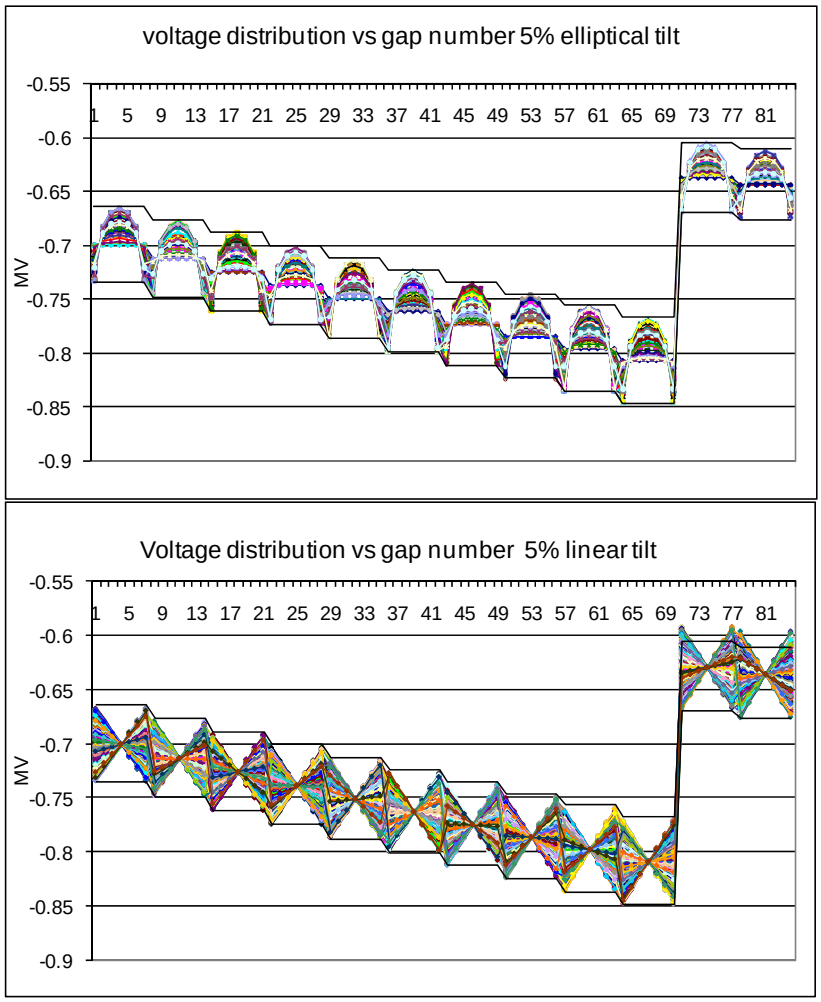

Figure 14 : Elliptical tilt (top), Linear tilt (bottom)

Table 10 : Effects on the longitudinal emittance of an elliptical or linear tilt in the PIMS

	Kinetic Energy Average [MeV]	90% Emittance [deg MeV]	RMS Emittance [deg MeV]	Kinetic Energy Standard Deviation [keV]
nominal	159.4279	0.7403	0.1804	85.0634
elliptical tilt 2%	159.310 ± 0.080	0.7423 ± 0.0006	0.1807± 0.0002	84.928 ± 0.551
elliptical tilt 5%	159.134 ± 0.093	0.7447 ± 0.0012	0.1811 ± 0.0002	84.676 ± 0.604
elliptical tilt 10%	158.838 ± 0.128	0.7486 ± 0.0021	0.1818 ± 0.0003	84.245 ± 0.745
linear tilt 2%	159.419 ± 0.078	0.7411 ± 0.0007	0.1805 ± 0.0002	85.043 ± 0.639
linear tilt 5%	159.415 ± 0.079	0.7412 ± 0.0014	0.1805 ± 0.0004	85.127 ± 0.986
linear tilt 10%	159.421 ± 0.082	0.7414 ± 0.0026	0.1806 ± 0.0008	85.1512 ± 1.700

Note the nominal longitudinal emittance out of the PIMS is few percent lower than the one out of the CCDTL. This is due to transverse-longitudinal emittance exchange in the PIMS.

4. Summary tables of alignment error tolerances

The final result of the error studies on the effect of alignement is a table of tolerances to be used by survey and mechanical engineer as a guideline to design the positioning and alignment system. The values summarized below are based on the results of the beam dynamics simulations and extensive discussion with the drawing office engineers to find a suitable compromise and distribute sensibly the error budget amongst the different sources of errors.

The tolerances are given as a sigma, assuming a Gaussian error distribution for the ensemble. The value at one sigma should be interpreted as the target value for alignment, whereas the value at three sigmas is the hard limit. (e.g. for LINAC quadrupoles, we can accept a deviation up to ±0.3 mm for few quadrupoles). We always assume that the distribution of errors is around the nominal position.

	X,Y (1 sigma)	Roll (1 sigma)	Pitch and yaw (1 sigma)	Comments
Chopper line quadrupoles , bunchers, inline dump and chopper plates.	±0.1 mm	±1mrad	2mrad (probably even more)	Chopper plates are very critical the rest is more forgiving.
LINAC quadrupoles (DTL,CCDTL,PIMS)	±0.1 mm	±1mrad	2mrad (probably even more)	Critical for beam quality. We have 1 corretor / 40 quadrupoles in the DTL. Less critical in CCDTL and PIMS.
Transfer lines quadrupoles	±0.2 mm	±2mrad	2mrad (probably even more)	
Steeres and dipoles	±0.5 mm	±2mrad	2mrad (probably even more)	
Diagnostics	±0.5 mm	Not relevant	Not relevant	For any passive element it is important to know the position but not necessarily to align, provided of course it doesn't influence the acceptance of the lines, see below.

The following guidelines should be used to determine the position of the diagnostics elements:

for transformers and BLMs it is not needed to know position and angle;

for pickups the position of the electrical centre should be known within ±0.3 mm and the relative longitudinal position between two consecutive pick-ups should be known better than 0.3 mm but there is no need to know the angle;

for SEM grids, wire scanners, and the Feshenko monitor the position of the centre should be known within ±0.3 mm and the angle to a precision of 3-5deg.

5. Summary tables of RF error tolerances

The final result of the error studies on the effect of RF errors is a table of tolerances to be used as a guideline to design the low level RF system and define the tuning accuracy..
The values summarized below are based on the results of the beam dynamics simulations and extensive discussion with the RF team to find a suitable compromise and distribute sensibly the error budget amongst the different sources of errors.
The tolerances refer to uniform error distribution. It is assumed that the average of the error distribution is adjusted to the nominal value.

	Amplitude Jitter (Uniform)	Phase jitter (Uniform)	Static field error – (Uniform)	Field unbalance for coupled cavities
RFQ	±1%	n/a		n/a
MEBT bunchers	±1%	±1 deg	n/a	n/a
DTL	±0.5%	±0.5deg	±2%(random gap field error)	n/a
CCDTL	±0.5%	±0.5deg	±2% (tilt over 3 modules)	±5%
PIMS	±0.5%	±0.5deg	±5% (tilt)	Not investigated
Transfer line debuncher	±1%	±1 deg	n/a	n/a

6. Summary tables of magnetic field quality tolerances

These tolerances apply to all the quadrupoles in the LINAC. The tolerances refer to a Gaussian distribution cut at 3 sigmas, unless otherwise indicated.

Gradient integral error ±0.5 % (uniform)
Magnetic versus geometric axis: < ±0.1 mm 1 sigma for LINAC quadrupoles.
Magnetic versus geometric axis: < ±0.2 mm 1 sigma for transfer line quadrupoles
Harmonic content at 75% radius: Bn/B2 for n=3,4,...10 : < 0.01
Yaw/pitch: ±2 mrad 1 sigma
Roll: ±1 mrad 1 sigma

7. References

[1] M. Vretenar ed., LINAC4 technical Design Report, CERN-AB-2006-084 ABP/RF (2006).

[2] CONCEPTUAL DESIGN OF THE SPL II, A High Power Superconducting H- LINAC at CERN, 2006

[3] A. Perrin, J.-F. Amand, T. Muetze, "Travel User Manual"

[4] R. Duperrier, N. Pichoff, D. Uriot, "CEA Saclay codes review", ICCS Conference 2002, Amsterdam

[5] Bellodi, G ; Eshraqi, M ; Lallement, J B ; Lombardi, A M "Updated layout of the LINAC4 transfer line to the PS Booster (Green Field Option)", CERN-AB-Note-2008-036. - 2008. - 14 p.

[6] Garcia Tudela, M ; Bellodi, G ; Eshraqi, M ; Hein, L M ; Lallement, J B ; Lombardi, A ; Posocco, P A ; Sargsyan, E, " Updated end-to-end simulations of LINAC4 ", sLHC-Project-Note-0025; CERN-sLHC-Project-Note-0025.- Geneva : CERN, 2010 - 31 p.

[7] R. Duperrier, "Toutatis, a radio-frequency quadrupole code", Phys. Rev, Spec. Top. Acc. & Beams, December 2000.

[8] Los Alamos accelerator code group : http://laacg1.lanl.gov/

[9] L. Hein, A. Lombardi, "Update of the LINAC4-PSB Transfer Line", sLHC-Project-Note-0028; CERN-sLHC-Project-Note-0028. - Geneva : CERN, 2010 - 33 p.

[10] Lombardi, A M ; Lallement, J B ; Sargsyan, E ; Lanzone, S ; Bellodi, G ; Eshraqi, M ; Hadorn, B "Loss Control and Steering Strategy for the CERN LINAC4",AB-Note-2007-033 ; CERN-AB-Note-2007-033. - 2007. - 16 p.

[11] Bellodi, G; Lallement, JB; Lombardi, AM; Posocco, PA; Sargsyan, E "LINAC4 chopper line commissioning strategy,sLHC-PROJECT-Report-0037 ; CERN-sLHC-PROJECT-Report-0037. - 2010. - 33 p.

[12] N. Schwerg, "Linac4: Klystrons and Power Distribution", Presentation 27/05/2010,http://indico.cern.ch/getFile.py/access?contribId=6&resId=1&materialId=slides&confId=92168

[13] A.M. Lombardi, G. Bellodi, M. Eshraqi, F. Gerigk, J.-B.Lallement, S.Lanzone, E. Sargsyan, R.Duperrier, D.Uriot, "Beam Dynamics In LINAC4 At CERN", proceeding HB2008,Nashville, Tennessee, August25-29 , 2008..

[14] Posocco, P ; Garcia Tudela, M ; Lombardi, A , "CCDTL Power Splitting",sLHC-Project-Note-0024; CERN-sLHC-Project-Note-0024.- Geneva : CERN, 2010 - 7 p.